A detailed mathematical analysis of a model that couples the cell cycle and apoptosis

Gheorghe Craciun* Baltazar Aguda† Avner Friedman*

Abstract: The cell division cycle and apoptosis are key cellular processes deregulated during carcinogenesis. Recent work of Aguda and Algar suggests a modular organization of regulatory molecular pathways linking the cellular processes of division and apoptosis. We carry out a detailed mathematical analysis of the Aguda-Algar model to unravel the dynamics implicit in the model structure. In addition, we further explore model parameters that control the bifurcations corresponding to the aforementioned cellular state transitions.

Keywords: cellular processes models, molecular pathways, cell cycle, apoptosis

1 Introduction

It is now widely accepted in the cancer research community that the cell division cycle and the cell death program (called *apoptosis*) are key cellular processes deregulated during carcinogenesis. Enhanced cell proliferation can be due to increased cell cycling and/or inhibited apoptosis. Recently, Aguda and Algar (2003) reviewed and analyzed the regulatory molecular pathways linking these cellular processes. These authors suggested a modular organization of the complex networks and presented a corresponding kinetic model for the cellular state transitions from quiescence (non-dividing) to cell cycling, and eventually to apoptosis as the strength of extracellular signaling increases.

The modular structure of the Aguda-Algar model is shown in Figure 1. The lines that end with "$\dashv$" indicate that one module inhibits the other, and the lines that end with "$\rightarrow$" indicate that one module activates the other. The modules involved correspond to intracellular signaling, cell cycle, apoptosis, and a control node of transcription factors that stimulate the expression of cell cycle and apoptosis genes. The key transcription factors are suggested to be the proteins E2F-1 and c-Myc. The primary components of the cell cycle module are the enzymes called cyclin-dependent kinases, and the key players in the apoptosis module are the caspases. An example of a signaling pathway would

*Mathematical Biosciences Institute, Ohio State University. The first and third authors were supported by the National Science Foundation upon Agreement No. 0112050. The third author was also supported by the National Science Foundation Grant DMS-0098520.

†Department of Genetics and Genomics, Boston University School of Medicine.

be the Ras/MAPK pathway which is a cascade of activation involving protein kinases (Huang and Ferrel (1996)). This signaling pathway has been shown (Huang and Ferrel (1996)) to possess an ultrasensitive switch-like behavior as depicted in Figure 1.

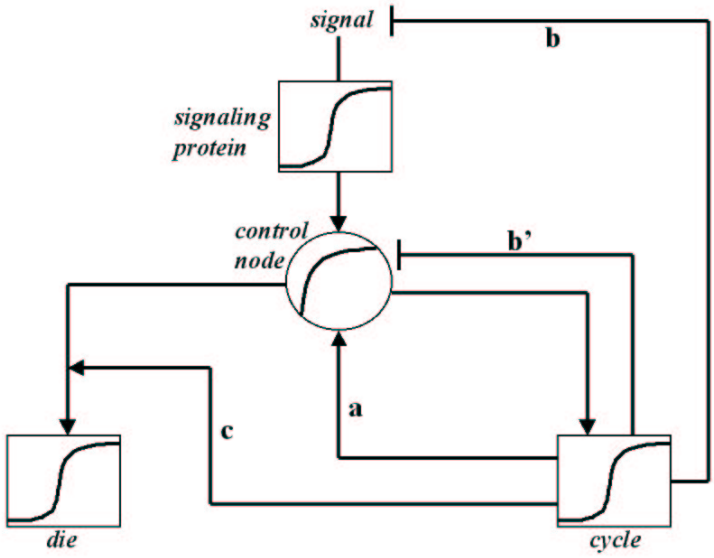

Figure 1: *Modular structure of the model.*

The interaction labeled "**a**" in Figure 1 represents the fact that activated cyclin-dependent kinases (e.g. CDK2) needed for entry into the cell cycle would further enhance the transcriptional activity of E2F-1 via phosphorylation of the retinoblastoma (Rb) protein. The interaction labeled "**b**" in Figure 1 represents the reported negative feedback between the Rb/E2F pathway and the Ras signaling pathway. The interaction labeled "**b'** " involves the negative regulation of cyclin A/CDK2 towards E2F-1 via the phosphorylation of the latter's partner, the DP proteins, which are required for binding DNA. Finally, the interaction labeled "**c**" would include the cell cycle-enhanced apoptosis via indirect regulation of caspases by cyclin-dependent kinases. More details and justification of these module-module interactions are discussed in Aguda and Algar (2003).

2 Description of the Model

A kinetic implementation of the modular model in Figure 1 is shown in Figure 2. The meaning of the notations used in Figure 2 is as follows:

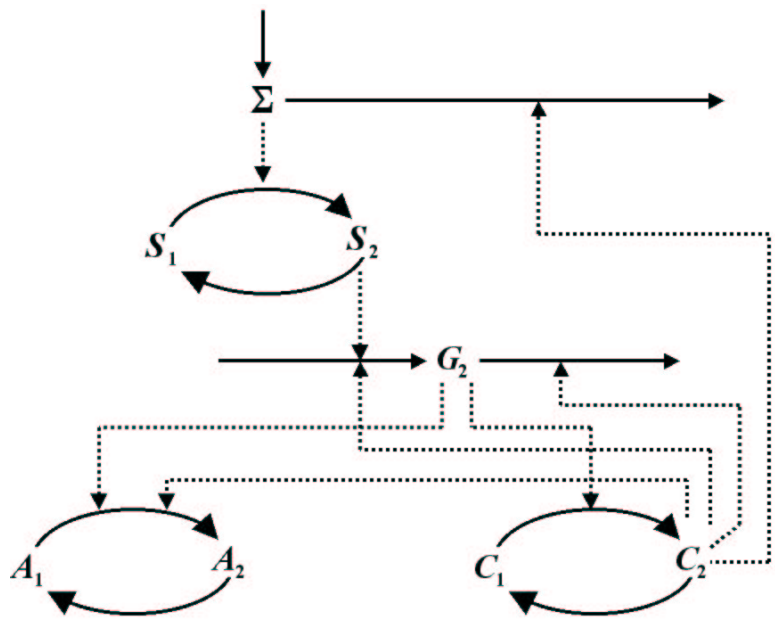

Figure 2: *Mechanistic implementation of the model. The solid arrows indicate input into or output from a node; dotted arrows indicate influence of a node on a process, without loss of mass.*

Σ = signaling molecule
S_2 = active signaling protein
G_2 = control node of transcription factors
C_2 = active cell cycle marker (for initiation of S-phase)
A_2 = active apoptosis marker

We will use the same species symbols for their corresponding concentrations. Then, according to either mass action or Michaelis-Menten kinetics we get the following system of differential equations:

$$\frac{d\Sigma}{dt} = \varepsilon^0(k_s - k_{sd1}\Sigma - k_{sd2}C_2\Sigma) \tag{1}$$

$$\frac{dS_2}{dt} = \varepsilon^{-2}\left(\frac{k_1\Sigma S_1}{K_{M1}+S_1} - \frac{v_{m1}S_2}{K_{Mr1}+S_2}\right) \tag{2}$$

$$\frac{dG_2}{dt} = \varepsilon^{-3}\left(k_2S_2 + k_{2a}C_2 - k_{m2}G_2 - k_{m2a}C_2G_2\right) \tag{3}$$

$$\frac{dC_2}{dt} = \varepsilon^{-1}\left(\frac{k_3G_2C_1}{K_{M3}+C_1} - \frac{v_{m3}C_2}{K_{Mr3}+C_2}\right) \tag{4}$$

$$\frac{dA_2}{dt} = \varepsilon^{2}\left(\frac{k_4G_2A_1}{K_{M4}+A_1} + \frac{k_{4a}C_2A_1}{K_{M4}+A_1} - \frac{v_{m4}A_2}{K_{Mr4}+A_2}\right) \tag{5}$$

Except for the time scaling factor ε, equations (1)-(5) are identical to those used in Aguda and Algar (2003). The cyclic reactions shown in Figure 2 - namely, those between the pairs of species $(S_1, S_2), (C_1, C_2)$, and (A_1, A_2) - imply that the total concentrations of each pair of species is constant. The individual reaction steps in these cyclic reactions are assumed to possess the Michaelis-Menten type of kinetics, i.e., the reaction rate has the form $vX/(K_M+X)$ where X is the substrate (reactant), v is the maximum reaction rate and K_M is the Michaelis constant. The maximum rate v is itself proportional to the enzyme catalyzing the step; e.g., for the conversion of S_1 to S_2, v is proportional to Σ since the latter is the catalyst for this step. In (1) and (3) the interactions take place by mass action law and degradation. For example, the term $k_{m2a}C_2G_2$ in (3) is due to degradation promoted by C_2, and the term $k_{m2}G_2$ is due to intrinsic degradation.

We include the various powers of ε to account for the fact that the various processes have different time scales. For negative powers of ε, the smaller the value of ε, the faster the process approaches equilibrium. For positive powers, small ε means that the evolving variable (e.g. A_2) changes very slowly. Thus, for example, in the subsystem (2)-(4), the variables S_2, G_2, C_2 are fast evolving, and G_2 and S_2 evolve faster than C_2, as suggested by the parameter values in Aguda and Algar (2003).

We take the parameter reference values (*p.r.v.*) to be: $k_s = 0.002$, $k_{sd1} = 0.001$, $k_{sd2} = 0.05$, $k_1 = 10$, $v_{m1} = 1$, $K_{M1} = K_{Mr1} = 0.02$, $k_2 = 0.1$, $k_{2a} = 0.01$, $k_{m2} = 1$, $k_{m2a} = 0.001$, $k_4 = 1$, $k_{4a} = 1$, $v_{m4} = 1$, $K_{M4} = 0.02$, $K_{Mr4} = 0.1$, $\varepsilon = 0.1$ and $S_1 + S_2 = 1$, $C_1 + C_2 = 1$, $A_1 + A_2 = 1$. For these *p.r.v.*, the time scale is such that one cell cycle typically takes 50-100 time units.

Except for ε, all other parameters are of the same order of magnitude as those chosen by Aguda and Algar (2003). Our aim is to show that the model is sufficient to account for the following experimental observations (see Evan and Vousden (2001); Blagosklonny (1999); Yamasaki et al. (1996)):

> *If the signal rate k_s is small then the cell is quiescent; if k_s is of intermediate size then the cell is cycling; and if k_s is large then the cell goes into apoptosis.*

We are assuming that there exists a threshold on the apoptosis marker beyond which apoptosis occurs irreversibly; without loss of generality, we suppose that apoptosis occurs when $A_2 > A_1$, i.e., $A_2 > \frac{1}{2}$.

Note that, for small ε, the process (3) reaches equilibrium much faster than the processes (1), (2), (4), and (5). Thus we may suppose that in the time it takes the variable G_2 to reach equilibrium the change in the other variables is negligible. Therefore, we may equate the right-hand side of (3) to zero and determine G_2 as a function of S_2 and C_2. Similar fast-slow variable considerations apply to the remaining equations, and they help us determine some rate parameters in our computations as we work with the full dynamical system.

The computational results that will be described here for $\varepsilon = 10^{-1}$ have been validated also for smaller values of ε, i.e., $\varepsilon = 10^{-2}$, $\varepsilon = 10^{-3}$, and $\varepsilon = 10^{-4}$.

3 Hysteresis loop for signal/cycle interplay

In order to get started we consider first the processes (2) and (3) which are the fastest processes within the system (1)-(4) for small ε. We first equate the right-hand side of (3) to zero and we solve for G_2 as a function of S_2 and C_2. Then we equate the right-hand side of (2) to zero and solve for S_2 as a function of Σ and C_2. Note that although in general this last equation has two solutions, only the one given by the Goldbeter-Koshland function is biologically relevant (the other solution would lead to a negative value for S_1, see Tyson et al. (2003); Goldbeter and Koshland (1981)).

Then (4) reduces to an equation

$$\frac{dC_2}{dt} = \Psi(C_2, \Sigma). \tag{6}$$

Equations (1) and (6) capture the dynamics of (1)-(4) restricted to the manifold obtained by making the right-hand sides of (2) and (3) equal to zero, and they represent a good approximation of the dynamics of (1)-(4) for small ε.

The nullcline of (6) has the S-shaped form shown in Figure 3. The upper

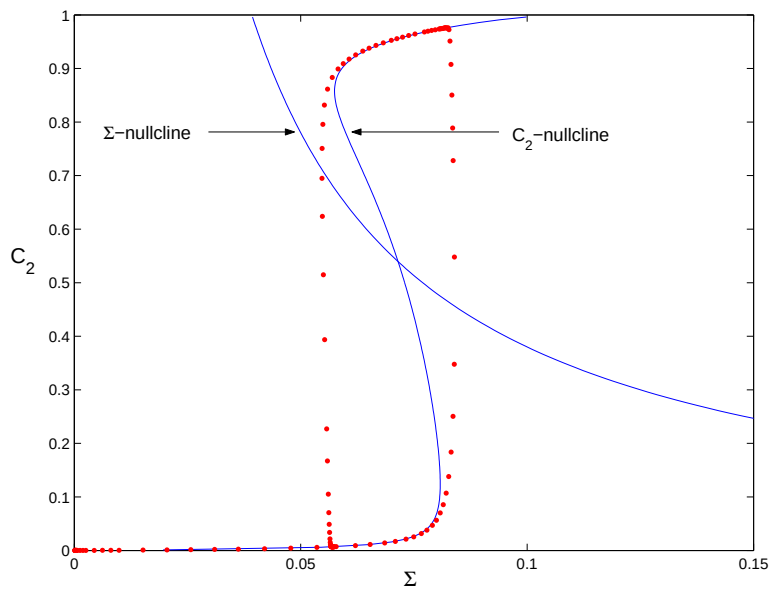

Figure 3: *The projection of the trajectory on the* (Σ, C_2) *plane, at p.r.v.*

and lower branches of the S-shaped curve are stable, and the middle branch is unstable. This suggests that, if the nullcline of (1) intersects only the middle branch, then as Σ increases to some critical value Σ_2 there is an upward jump (which can be interpreted as having crossed the checkpoint for cell cycle entry),

and when the signal is decreased to some critical value Σ_1 the cell gets back to its initial (post-mitotic) phase.

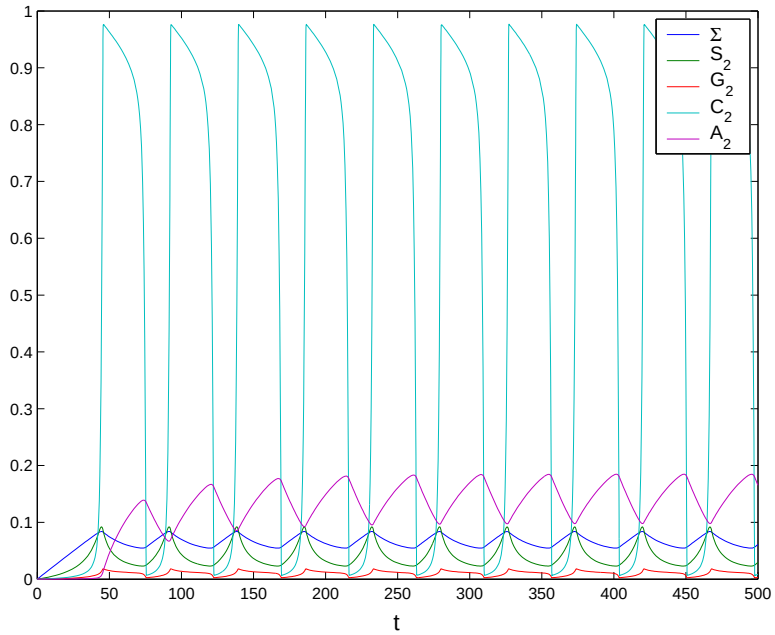

Figure 4: *Solutions of (1)-(5) as explicit functions of time at p.r.v.*

We shall now describe our computational results for the full system (1)-(5). The initial values are $\Sigma = S_2 = G_2 = C_2 = A_2 = 0$.

First, for the *p.r.v.*, we get the results in Figures 3 and 4. The curve spanned by dots in Figure 3 is the projection of the solution on the (C_2, Σ)-plane. The S-shaped C_2-nullcline in Figure 3 is the curve $\Psi(C_2, \Sigma) = 0$, i.e., for each fixed Σ we compute C_2 by solving (2), (3), (4) at equilibrium. Figure 4 shows the *periodic* behavior of all the components of the solution of (1)-(5) after some time (approx. 100 time units). Note that $A_2 < \frac{1}{2}$, so the cell does not go into apoptosis.

The nullcline of (1) is determined by the equation

$$\Sigma = \frac{k_s}{k_{sd1} + k_{sd2} C_2}. \tag{7}$$

This Σ-nullcline varies with the parameters k_s, k_{sd1}, and k_{sd2}. In particular, as we vary the signal input rate k_s (and keep all the other parameters fixed) the Σ-nullcline changes, but the C_2-nullcline does not.

If, roughly, $k_s < 0.00065$, and all other parameters are at *p.r.v.* then the two nullclines intersect below the lower knee of the S-shaped C_2-nullcline, and

the cell is quiescent (see Figure 5). In this case the cell "gets stuck" at the intersection of the nullclines of Σ and C_2 before reaching the lower knee of the S-shaped curve. This is a quiescent cell, with $A_2 < \frac{1}{2}$ (no apoptosis).

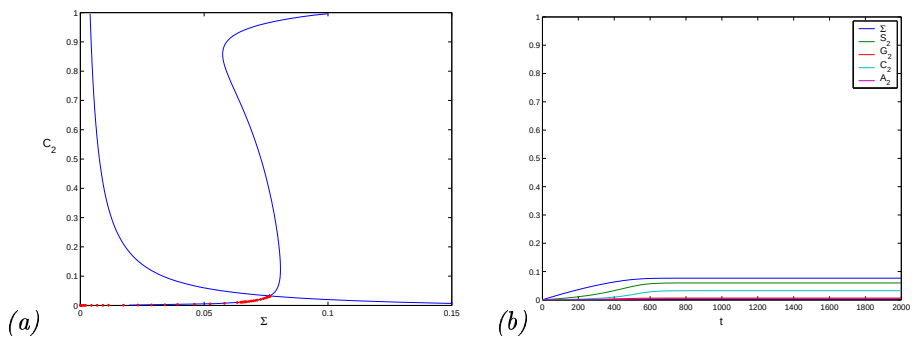

Figure 5: $k_s = 0.0002$*: (a) reduced phase plane (b) explicit functions of time.*

If $k_s > 0.00251$ then the two nullclines intersect above the higher knee of the S-shaped C_2-nullcline (see Figure 6). The variable C_2 jumps up (i.e., the cell crosses the checkpoint for cell cycle entry), but it does not complete the cycle: it "gets stuck" at the intersection of the two nullclines. In this case $A_2 > \frac{1}{2}$ after about 350 time units, i.e., the the cell enters apoptosis.

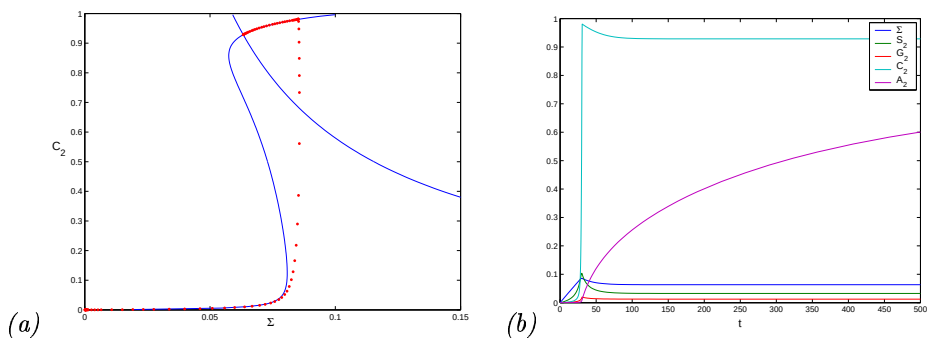

Figure 6: $k_s = 0.003$*: (a) reduced phase plane, (b) explicit functions of time.*

For $k_s = 0.00065$ the two nullclines intersect just above the lower knee of the C_2-nullcline (see Figure 7(a)), and for $k_s = 0.00251$ they intersect just below the higher knee (see Figure 8(a)). In both cases the cell is cycling. However, as shown in Figures 7(b) and 8(b), for k_s just above the quiescent limit the cell spends most time in the passive stage (i.e., $C_2 \approx 0$), and for k_s just below the apoptotic limit the cell spends most time in the active stage (i.e., $C_2 \approx 1$).

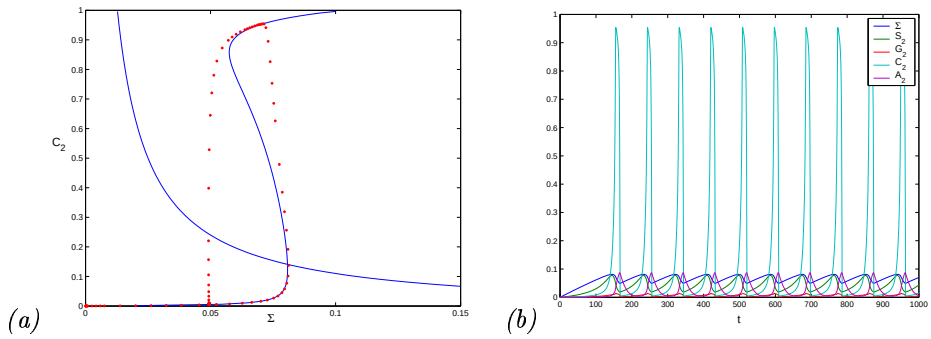

Figure 7: *k_s is near the quiescent limit: (a) reduced phase plane (b) explicit functions of time.*

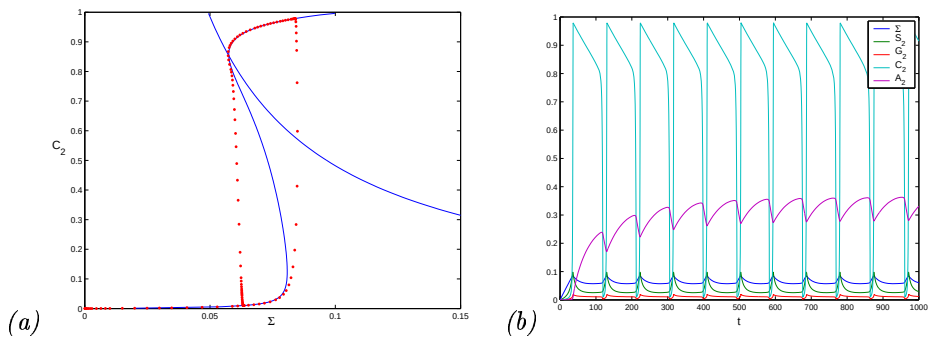

Figure 8: *k_s is near the apoptotic limit: (a) reduced phase plane (b) explicit functions of time.*

4 The role of other parameters

The choice of parameter reference values is important for our results. We consider here some examples where we vary some of the other parameters.

Consider the parameter k_{2a}, related to the input provided by the cell cycle marker C_2 to the control node G_2. This parameter measures the "depth" of the hysteretic loop of the C_2-nullcline. If we increase k_{2a} from its reference value 0.01 to $k_{2a} = 0.012$ we get a "deeper" C_2-nullcline, as we see by comparing the C_2-nullclines from Section 3 with the C_2-nullcline in Figure 9(a). On the other hand, if we decrease k_{2a} then the "depth" of the S-shape decreases. In particular, if $k_{2a} = 0$ then the C_2-nullcline loses its S-shape, so we cannot get a hysteretic loop (see Figure 10). In this case the solution, instead of being periodic, converges to some fixed point at the intersection of the nullclines.

We shall now consider the case where $k_{2a} = 0.012$. If we keep all the other parameters at their reference values then, as seen in Figure 9(a), the cycle

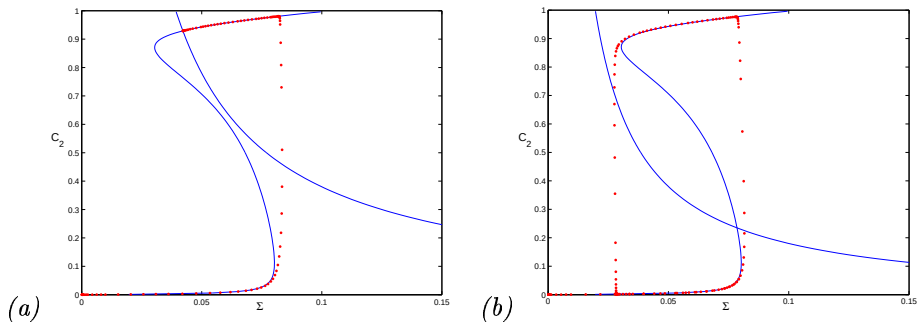

Figure 9: $k_{2a} = 0.012$: (a) for k_s at its reference value (b) for $k_s = 0.001$, smaller than its reference value.

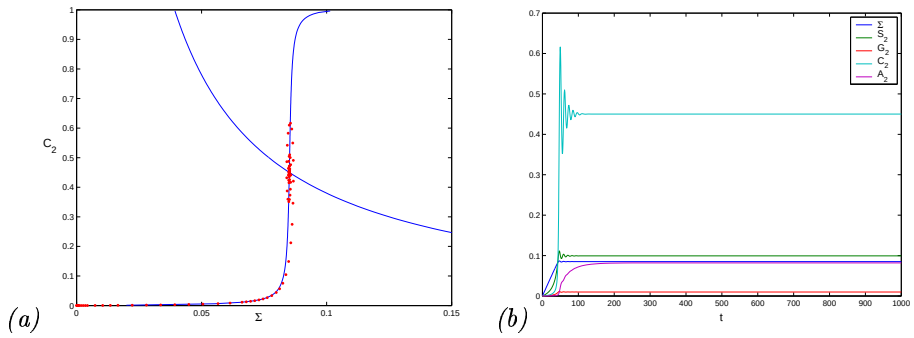

Figure 10: *The case $k_{2a} = 0$: (a) reduced phase plane (b) explicit functions of time.*

begins its upward jump, but does not come down to completion, since the intersection between the two nullclines is now on the upper branch of the C_2-nullcline. Therefore the cell goes into apoptosis ($A_2 > \frac{1}{2}$ after some time). However, if k_s is decreased (from the reference value $k_s = 0.002$ to $k_s = 0.001$), then the cell goes into cycling (with $A_2 < \frac{1}{2}$) as shown in Figure 9(b).

If k_{2a} becomes very large then the two nullclines will always intersect along the stable upper branch of the S-shaped nullcline, and the trajectory will get "stuck" at that stable fixed point. In this case we can only have quiescence or apoptosis (i.e., in this case there can be no cycling for any values of k_s and k_{sd2}).

Finally, let us look at the interplay between the parameters k_{sd1}, k_{sd2}, and k_s. The three possible modes of the cell are summarized in the diagrams of Figure 11. The equation of the lower line in Figure 11(a) is determined by the condition that the Σ-nullcline passes exactly through the lower knee of the S-shaped curve (i.e., the lower knee of the C_2-nullcline). Similarly, the equation

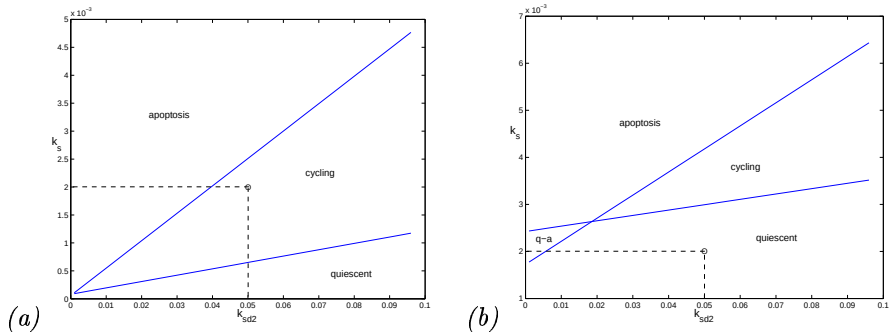

Figure 11: *The mode diagram: (a)* $k_{sd1} = 0.001$ *(b)* $k_{sd1} = 0.03$. *The special points are the p.r.v. for* k_s *and* k_{sd2}

of the higher line in Figure 11(a) is determined by the condition that the Σ-nullcline passes exactly through the higher knee of the C_2-nullcline. If k_{sd1} is very small (e.g., $k_{sd1} = 0.001$, its reference value) then it is roughly the quotient k_s/k_{sd2} that determines the mode (see Figure 11(a)). As we increase k_{sd1} both lines are raised, but the lower line is raised faster than the higher line. Hence, the cycling region shifts upward and at the same time decreases (see Figure 11(b)), and a new region of quiescence appears between the two lines. For example, if all parameters are set at their reference values, except for $k_{sd1} = 0.03$, then the cell is quiescent as in Figure 5, instead of cycling as in Figures 7 and 8.

5 Conclusions

It has been shown experimentally (Evan and Vousden (2001); Blagosklonny (1999); Yamasaki et al. (1996)) that there is an optimum range of transcriptional activities for E2F-1 and c-Myc for cells to proliferate. If the intensity of growth factor signaling is too small, cells are quiescent and do not cycle. However, if signals are too large then the apoptosis program is triggered; this can be interpreted as an important failsafe mechanism to prevent uncontrolled cell proliferation as it occurs in cancer.

In this paper we have analyzed a simple model (developed by Aguda and Algar (2003)) and established the above biological observation for a certain range of parameters within the network. We also investigated what happens as one goes beyond this range of parameters.

We have shown that the positive feedback loop (shown as "**a**" in Figure 1) is required for an S-shaped C_2-nullcline. This nullcline geometry is essential for a switch-like behavior between the various cellular states, particularly from quiescence to cell cycling and/or apoptosis. The positive loop "**a**" is represented by a nonzero value of the parameter k_{2a} in the Aguda-Algar model. The biochemical basis of this loop is well established (Aguda and Algar (2003)); the

transcriptional activities of the factors E2F-1 and c-Myc (represented by G_2 in the model) are increased by CDK2 (represented by C_2 in the model) via inhibition of the retinoblastoma protein (Rb) which inhibits the G_2 factors. Our analysis suggests that the parameters involved in this positive feedback loop are the key parameters for controlling the cellular state transitions. Our simulations on the effect of signal strengths are consistent with experimental reports on the induction of apoptosis (Aguda and Algar (2003)).

The cross-shaped phase diagram in Figure 11(b) is an interesting result. The diagram shows that the series of cellular state transitions depends on the magnitude of the negative feedback loop between C_2 and the signal Σ (as measured by the value of k_{sd2}). For example, if the signal rate k_s is increased while keeping $k_{sd2} = 0.05$, then the system goes from quiescence to cycling, and eventually to apoptosis. But for k_{sd2} below 0.02, say $k_{sd2} = 0.01$, the same increase in k_s will not give rise to an intermediate cell cycling state. The region denoted by "**q-a**" is a region where the cell could either be quiescent or apoptotic depending on the cells history. If the cell is previously quiescent and the signal increases to the "**q-a**" region, then the cell remains quiescent; however, a further increase in the signal will send the cell directly into apoptosis (without going through the intermediary cell cycle phase). Thus, we predict that, if the negative feedback loop between the cell cycle and signaling pathways that impinge on the E2F-1/c-Myc node is very weak (namely, k_{sd2} is small), then for large enough signal degradation rate (k_{sd1}), the cell will bypass the cycling phase as it goes (with increasing signal input rate k_s) from quiescent phase to apoptosis.

It would be interesting to extend the model to a more realistic network which includes the key components of the cell cycle module such as Rb, cyclin E/CDK2, Cdc25A and p27Kip1 (see Aguda and Algar (2003)). It would also be interesting to include in the model details of the apoptosis module that incorporate a positive feedback loop between executioner caspases and cytochrome c release, also reviewed in Aguda and Algar (2003).

References

Aguda B.D. and C.K. Algar (2003). A structural analysis of the qualitative networks regulating the cell cycle and apoptosis. Cell Cycle 2, 538-544.

Blagosklonny M.V. (1999). A node between proliferation, apoptosis and growth arrest. BioEssays 21, 704-709.

Evan G.I. and K.H. Vousden (2001). Proliferation, cell cycle and apoptosis in cancer. Nature 411, 342-348.

Goldbeter A. and D.E. Koshland Jr. (1981). An amplified sensitivity arising from covalent modification in biological systems. Proc. Natl. Acad. Sci. USA 78, 6840-6844.

Huang C.Y.F. and J.E. Ferrell Jr. (1996). Ultrasensitivity in the mitogen-activated protein kinase cascade. Proc. Natl. Acad. Sci. USA 93, 10078-10083.

Tyson J.J., K.C. Chen and B. Novak (2003). Sniffers, buzzers, toggles and

blinkers: dynamics of regulatory and signaling pathways in the cell. Curr. Opin. Cell Biol. 15, 221-231.

Yamasaki L., T. Jacks, R. Bronson, E. Goillot, E. Harlow and N.J. Dyson (1996). Tumor induction and tissue atrophy in mice lacking E2F-1. Cell 85, 537-548.